International Journal for Housing Science and Its Applications
Publish August 10, 2025. Volume 46, Issue 4 Pages 1832-1842

https://doi.org/10.70517/ijhsa464159

Numerical simulation analysis of the power generation transfer characteristics of graphene-cobalt composite material-modified microbial fuel cell anodes

Feng Deng[1,*]
[1] Guangzhou Panyu Polytechnic, Guangzhou, Guangdong, 510220, China
Corresponding authors: (e-mail: marcoisdf@hotmail.com).

Abstract In order to understand the transfer characteristics of graphene cobalt composite modified microbial fuel cell anode electricity generation, it was analyzed by numerical simulation. In this paper, simulation experiments are designed to test the microbial fuel cell anode power generation characteristics by algal MFC constitutive chamber, and the microbes in the fuel cell are analyzed by electrochemical analysis test methods. 2 weak peaks are present in the CF electrode, which correspond to the D and G peaks, respectively. 4 peaks are present in the PPy-CF electrode, and there is a PPy-like substance attached on the surface of the electrode. rGO/PPy-CF electrode and GO/ PPy-CF electrode both had graphene and polypyrrole present on the surface. The charge transfer resistance of each anode increased after biofilm formation. Among them, CG-1000 had the highest conductivity and possessed the best electron transfer performance. The CG anode exhibited higher current density. The MFC degradation rates of the R/CC, R+GNS/CC, R+MWCNT/CC, and R+GNS+MWCNT/CC-modified anodes were 9.0, 11.5, 12.5, and 15 mg/h, respectively, and the output voltages were stable at 47, 77, 122, and 230 mV. The extracellular proteins and DAN of microorganisms were increased and polysaccharides were decreased in the anodes of R+GNS/CC, R+MWCNT/CC, and R+GNS+MWCNT/CC, and the MFC power-producing performance was improved.

Index Terms algal MFC, graphene-cobalt composite, microbial analysis, battery anode, MFC power production

I. Introduction

Microbial fuel cell (MFC) is a new technology that generates electricity while purifying wastewater, which is a device that uses microorganisms to convert biomass into electricity, and has great potential for application in wastewater treatment, microbial sensors, seawater desalination, and electrolysis for hydrogen production, etc., however, the low output power density restricts the application of the microbial fuel cell in practice [1]-[4]. In recent years, the research on microbial fuel cells has focused on the improvement of configuration, optimization of operating conditions, exploration of microbial power production mechanism, new electrode materials, etc. The development of high-performance anode materials is crucial to improve the power output of microbial fuel cells, and good anode materials require good electrical conductivity, biocompatibility and large specific surface area, etc. [5]-[8].

Traditional electrode materials for microbial fuel cells include carbon cloth, carbon felt, carbon paper, stainless steel mesh, etc., however, the electrocatalytic activity of the surface of ordinary carbon materials, as well as the electron transfer ability are poor, the electrons generated by the metabolic process of microbial bacteria to leapfrog to the electrodes of the ordinary carbon materials need to consume high energy, resulting in a larger anode activation overpotential In order to reduce the anode activation overpotential [9]-[12]. To further improve the power production performance of the battery anode, the surface of the ordinary carbon material electrode must be modified. Currently, graphene composites have been used in the modification of anodes for microbial fuel cells and significantly improved [13]-[15]. Graphene is a new carbonaceous material in which carbon atoms are tightly stacked into a single two-dimensional honeycomb lattice structure, which is the basic unit for constructing other carbonaceous materials, such as zero-dimensional fullerene, one-dimensional carbon nano-M tubes, three-dimensional graphite, etc., and it has many excellent and unique physical, chemical, and mechanical properties [16]-[19]. In modified microbial fuel cell anodes, the advantages of graphene composites mainly come from structural properties, high mechanical strength, and electrical conductivity [20], [21].

Literature [22] prepared graphene-cobalt/nickel composite carbon cloth (Gr-Co/Ni-CC) electrodes and graphene-cobalt/nickel composite carbon cloth electrodes, demonstrated by techniques such as energy dispersive x-ray (EDX), that the pleated graphene flakes and granular Co/Ni composites were successfully loaded on the surface of the carbon cloth, and revealed that Gr-Co/Ni-CC anodes are an effective choice for improving the performance of

MFC. Literature [23] illustrated that graphene-modified materials can improve the power generation performance of microbial fuel cells (MFCs) and reviewed graphene-modified electrode synthesis methods such as graphite oxide reduction and self-assembly methods, pointing out that graphene-modified electrodes are expected to solve the problem of low efficiency in spite of the many challenges faced by MFC electrodes. Literature [24] introduced graphene and its applications, pointing out that graphene-based anodes can improve MFC performance and electron transfer efficiency, while in the cathodic process, graphene-based materials can effectively catalyze the oxygen reduction reaction. Literature [25] described the advantages of microbial fuel cell (MFC) technology and the problems it poses, and investigated the use of graphene derivatives (L-GO) derived from oil palm biomass waste for the anode of a MFC with dual chambers, and the experimental results revealed that the oil palm biomass is an effective and low-cost material that can be used to improve the anode performance of MFCs. Literature [26] analyzed the potential of graphene oxide (GO) composite porous tetrahedral zeolite clay as an excellent biocompatible anode material for MFCs, showing that the high specific surface area of graphene oxide contributes to the extensive support of the zeolite capping layer, which improves the performance of MFCs. Literature [27] discussed the effect of graphene-related composites on the performance of MFCs and microbial electrolytic cells (MECs), providing a reference for selecting suitable graphene materials for modifying MFC and MEC electrodes to improve performance. Literature [28] points out that the conversion of chemical energy contained in organic matter into electrical energy is a topic of wide interest at present and describes the application of this technology in MFCs, as well as the selection of techniques and attempts by scientists around the world to use graphene in MFCs and their results. Literature [29] prepared graphene/Fe2O3 (G/Fe2O3) modified anode by one-step hydrothermal reduction method aiming to improve the performance of MFCs, and verified that the G/Fe2O3 material has good biocompatibility. Literature [30] electrochemically deposited two doses of reduced graphene oxide and composites of rGO and Fe(III) in a two-chamber MFC fueled by wastewater in order to improve MFC power generation, identified 12 bacteria supporting voltage, current and power generation in MFCs, and revealed the correlation between power production and citric acid cycle. Literature [31] discusses the recent research and applications of carbon nanotubes, graphene, graphitic carbon nitride and their composites as MFC anode/cathode and reviews the characteristics, modification/preparation methods and performance of MFC.

In this paper, in order to simulate the transfer characteristics of graphene-cobalt composites in the anodic power generation process of modified microbial fuel cells, simulation experiments were designed to construct algal MFCs, and the MFC reactor was used to analyze the performance of the microbial fuel cell anode power generation characteristics such as the output voltage, polarization curves, electrode potential curves, and the Coulomb efficiency. The performance of the fuel cell was analyzed by cyclic voltammetric curve, linear cyclic voltammetry, and AC impedance method. Finally, the extracellular electron transfer mechanism of CGs anode MFCs, the effect of modified anode on perchlorate reduction, MFC power generation performance and the EPS analysis of microorganisms attached to modified anode were further discussed based on the experimental data.

II. Experimental component

II. A.Preparation of graphene oxide

Graphene oxide (GO) was prepared by the modified Hummers method [32]. The specific synthesis method was as follows: Graphite scales (3.0 g) and potassium permanganate (18.6 g) were slowly dispersed into 360 mL of concentrated sulfuric acid, and then added to the mixed acid (360 mL of concentrated sulfuric acid + 40 mL of concentrated phosphoric acid), at which time the system was heated to 35-40 °C, and then stirred at a constant temperature after the water bath was heated up to 50 °C for 12 h. The reaction system was cooled to room temperature, poured into an ice-water mixture (400 mL) The reaction system was cooled to room temperature, poured into the ice-water mixture (400 mL), and added 15 mL of H2O2 (mass fraction 30%, the same as the whole text). At this time, the solution was changed from red to bright yellow with metallic luster, and left to precipitate for 2 h. The supernatant was washed with deionized water, hydrochloric acid (30% by mass), ethanol and centrifuged (11000 r/min, 30 min), and the above washing and centrifugation steps were repeated until the solution was neutral. The resulting GO was dried under vacuum at 60 ℃ for 24 h, and ground into fine powder for use.

II. B.Electrode Preparation

In a 250mL beaker A, GO was added to 50mL of deionized water and fully stirred to configure a solution (final concentration of 2g/L), then 10mL of 3mol/L hydrochloric acid was added to the beaker and continued to stir. Accurately weighed 14.55 g of Co(NO3)2-6H2O was poured into another 250 mL beaker B, and then 50 mL of deionized water was added and dissolved with sufficient stirring, and then poured into beaker A. The deionized water was replenished to 200 mL, and stirred sufficiently, to obtain an aqueous electrolyte solution with a final CO concentration of 0.1 mol/L. Place 1 piece of carbon felt electrode in the beaker C of the above electrolyte aqueous

solution, and then wrap the mouth of the bottle with a protective film and sonicate for 2 h. Subsequently, remove the electrode, fix it on the reaction device, wrap the beaker with tinfoil as a whole, and strictly avoid light. Add 1.7 mL of pyrrole to the beaker and stir magnetically for 30 min. pour the solution into the electrolytic cell, insert the glycocalyx reference electrode and platinum counter electrode, and apply a constant potential of 0.8 V using an electrochemical workstation with a running time of 600 s. The composite material polymerization was electrodeposited onto the surface of the carbon felt, and the GO/PPy/Co composite electrode was obtained. The electrode was removed and the surface adherents were rinsed slowly with deionized water. Meanwhile, PPy/Co and PPy electrodes were prepared according to the same procedure, and a blank carbon felt electrode was used as a control.

II. C. Construction of algal MFC

II. C. 1) Construction of algal MFCs

The algal MFC configuration used was a two-chamber configuration consisting of an anode chamber and a cathode chamber, both with a volume of 250 mL, separated by a cation exchange membrane. The cathode and anode were nickel foam (5 cm × 6 cm) connected to an external resistor through a titanium wire to form a circuit. During operation, the cathode and anode were connected to a 500Ω external resistor (except for testing the polarization curve).

II. C. 2) Inoculation and initiation

The Chlorella vulgaris used in this paper is a mixed bacterium, which comes from mixed anaerobic/aerobic sludge inoculated from sewage plants and domesticated in MFC.

(1) Cathodic and anodic electroactive biofilm domestication

The anode was inoculated with anaerobic sludge taken from the Hunter Wastewater Treatment Plant (WWTP), with a final inoculum of volatile suspended solids (VSS) at a mass concentration of 2 g/L. At the same time, glucose (electron donor), phosphate buffer (0.1 mol/L), metallic trace elements and multivitamins were administered to the anode and the anode chamber was replenished with deionized water, and the openings were sealed with a rubber stopper to maintain an anaerobic anode. The cathode inoculum source and nutrient medium were the same as that of the anode, only glucose was replaced with an inorganic carbon source, NaHCO3. Artificial aeration was applied to the cathode at an aeration rate of 30 mL/min. 500 Ω resistor was connected externally, and a data collector was used to monitor the voltages between cathode and anode, and replace the cathode and anode solutions when the voltages were reduced to 5% of the maximum voltage. To be continuously observed more than three cycles of repetitive stabilization of voltage generation, cathode and anode electroactive biofilm cycle is completed.

(2) Algae biological domestication

Remove cathode aeration and add pre-cultured Chlorella in logarithmic growth phase to the cathode, inoculated at 20% of cathode volume. At the same time, the algae/bacteria composite nutrient medium was added to the cathode. An artificial light source (light intensity of 3000lx) was applied to the cathode and the dark/light cycle was controlled to be 12h/12h.

The algae/bacteria MFC was operated normally under the conditions of the second step above and the related indexes were tested.

II. D. Characterization and analysis methods

Surface morphology analysis of different electrodes was performed using a scanning electron microscope (SEM, XL-30, Philips, Netherlands). Prior to observation, the electrodes were dried at 60°C in an oven. Cyclic voltammetry (CV) and electrochemical impedance spectroscopy (EIS) were conducted using an electrochemical workstation (Model 2273, Princeton, USA). CV was performed using the standard three-electrode configuration, with the working electrode as the anode, the counter electrode as the cathode, and the Ag/AgCl electrode as the reference electrode, at a scan rate of 25 mV/s. The AC signal amplitude for EIS was 10 mV, with a frequency range of 10 kHz to 5 mHz. All tests were conducted under open-circuit conditions. When measuring anode impedance, the anode served as the working electrode and the cathode as the counter electrode; when measuring cathode impedance, the roles were reversed. In both cases, the Ag/AgCl electrode served as the reference electrode (with a potential of +0.195 V relative to the standard hydrogen electrode).

III. Reactor start-up and test methods

III. A. MFC Startup

At all stages of reactor inoculation, incubation, domestication, and operation, the substrate for MFC was prepared from phosphate buffer solution at a concentration of 50 mM, in which 1 g L-1 of sodium acetate was used as the main substrate, and vitamins were added at 2 mL L-1, and trace elements at 1.25 mL L-1, in order to promote the growth of microorganisms. The inoculum was obtained from domestic wastewater from the municipal network on

campus, and the domestic wastewater was mixed with sodium acetate and inoculated continuously at 50%, 20%, and 10%. The substrate was replaced every 24 h during the initial cycle. After current generation, the substrate was replaced when the signal of the data acquisition card was lower than 50mV, and the inoculation was stopped after stabilizing the output voltage, and the initial MFC was started at 35℃, and the incubation temperature was precisely controlled by the constant temperature incubator. If not specified, the external resistance value is 1000Ω.

III. B. Output Voltage

The single-compartment MFC reactor was connected to the external resistance through a wire, and the cathode and anode formed a closed loop, and the output voltage was recorded by a computer through a data acquisition card (PISO-813, ICP DAS), which was automatically collected every 1 min and averaged every 30 min, and the range of the voltage was set to be 0~2.5 V in this experiment.

III. C. Power density

The goal of an MFC reactor is to obtain maximum output power [33] and maximum current density at the highest potential. The power density curve characterizes the change in power density with increasing current density, and researchers usually indicate the highest point of the power density curve as the maximum power obtained by the system. The current density (i) is the current per unit area, which is calculated as equation (1), and the power density is obtained by current density calculation. The power density curve is measured by gradient reduction of resistance, firstly, the system is opened to a stable state, while the open circuit voltage at both ends of the MFC is recorded, and the gradient external resistance values of 3000, 2000, 1000, 900, 800, 700, 600, 500, 400, 300, 200, 100, and 50 Ω are selected for the measurement in turn, and after the MFC reactor is stabilized, the following are recorded voltage at both ends of the anode and cathode, and calculate the output power based on equation (2):

$$i = I / S \tag{1}$$

$$P = i \times U \tag{2}$$

III. D. Polarization curves

Polarization curve is used to represent the relationship between current density and output voltage, by changing the value of external resistance, the corresponding voltage and the current value under this resistance value are obtained. The polarization curve represents the voltage obtained by MFC under a certain current, and the gradient external resistance values are selected in order to measure 3000, 2000, 1000, 900, 800, 700, 600, 500, 400, 300, 200, 100, 50Ω in order, and the output voltage needs to be stabilized for 30min after replacing the resistor and then recorded.

III. E. Electrode potential curves

The electrode potential curve can be used to fully analyze the system performance of the MFC, and the electrode internal resistance can be derived from the slope of the straight line portion of the electrode potential curve. The electrode potential curve is used to represent the change of electrode voltage with the increase of current density, and a number of gradient resistance values of 3000, 2000, 1000, 900, 800, 700, 600, 500, 400, 300, 200, 100, 50Ω are selected, and the cathode and anode potentials are measured sequentially after stabilization.

III. F. Cullen efficiency

The Coulomb efficiency is the ratio of electrical energy converted by the oxidative release of electrons from the metabolized substrate by anodic microorganisms to the theoretical electrical energy converted by the oxidative release of electrons from the substrate [34]. The main reasons for keeping the Coulomb efficiency low are: firstly, the substrate is oxidized by air and less utilized by the anode microorganisms; and secondly, limiting the cathode's oxygen reduction process reduces the current. Both will result in lower Coulomb efficiency, which is calculated as equation (3):

$$CE = \left\{ M \int_0^T Itdt \right\} \Big/ \left(nVF\left(COD_0 - COD_T \right) \right) \tag{3}$$

where, M - the molecular weight of oxygen; T - the time taken by the MFC to run a single cycle; n - the number of electrons gained per unit mole of oxygen being reduced; COD_0 - initial COD value of the anode substrate; COD_T - COD value of the anode substrate after running a single cycle; V - volume of the anode substrate; F - - the Faraday constant (96485 C mol^{-1}).

IV. Electrochemical analysis test methods

IV. A. Cyclic Voltammetry

Cyclic voltammetry was determined using an electrochemical workstation, where the electrode potential was set and continuous scans were performed at different scanning rates of 1 mV s^{-1}, 5 mV s^{-1}, and 10 mV s^{-1}, in both forward and reverse directions, and the potential returned to the initial value, which is considered cyclic. In this study, the electrodes were tested in order to examine the anodic biofilm activity at different temperatures. During scanning, saturated calomel, anode carbon brush and cathode were tested as reference electrode, working electrode and counter electrode, respectively, with the scanning range of +0.5V to -0.5V, respectively, before the substrate was consumed and before the substrate was completely degraded in two cases, and each scanning was performed for four cycles until the curves were completely overlapped, and the results of the last curve were taken and analyzed.

IV. B. Linear cyclic voltammetry

Linear cyclic voltammetry involves scanning in a set direction at a fixed scan rate and recording the change in potential at the working electrode. An electrochemical workstation was used in this study to examine the parallelism of the air cathode. In the experiment, air cathode, Pt slice (1 cm^2) and saturated mercuric glycol were used as working electrode, counter electrode and reference electrode, respectively, and the test medium was 50 mM phosphate buffer solution with a scanning range of -0.3 V to 0.3 V and a scanning rate of 1 mV s^{-1}, and each slice was scanned four times until the LSV curves were completely overlapped, and the results of the last one were taken for analysis.

IV. C. AC impedance method

The electrochemical AC impedance method is realized based on the signal overlap of the sinusoidal curves of tiny currents at the working electrode [35]. In the test, the frequency of its sinusoidal signal is varied within a certain range and the electrode impedance is plotted to obtain the internal resistance. In this experiment, the internal resistance of the anode biofilm was tested using an electrochemical workstation with a carbon brush as the working electrode, a saturated calomel electrode as the reference electrode, and a Pt/C air cathode as the counter electrode. A voltage of 0.2 V was applied with a scanning frequency of 100 kHZ to 10 mHZ and a perturbed sine wave amplitude of 5 mV. The test was performed using the electrochemical workstation and the equivalent circuit was fitted using Nova 2.1. Each scan was performed 4 times until the curves were completely overlapped and the last result was taken for analysis.

V. Microbiological analysis

V. A. Morphological analysis of anode bacteria

The attachment of biofilm on the electrode surface could be visualized by scanning electron microscopy. The pretreatment of the samples was as follows: firstly, the obtained electrode samples were immersed in 2.5% glutaraldehyde solution and kept at 4°C for 2 h. Subsequently, the samples were dehydrated by using gradient ethanol solution for 10 min respectively, and then dried naturally at room temperature. The dehydrated samples were dried in air and subsequently observed the morphology of the biofilm under a scanning electron microscope.

V. B. Analysis of anode bacterial community structure

Sample DNA was up-sequenced on the NovaSeq 6000 sequencing platform after library construction and quantification according to the instructions of Beijing Novozymes Technology Co. The sequencing results were subjected to noise reduction using the DADA2 module in QIIME2 software to obtain the final amplicon sequence variants (ASVs) and characterization tables. Species annotation was performed for each ASV using the classify-sklearn algorithm of QIIME2 software and a pre-trained Naïve Bayes classifier, and the annotation database was Silva 138.1. Rapid multiple sequence alignment was performed using QIIME2 software to obtain the phylogenetic relationships of all ASV sequences and to construct a phylogenetic tree. Due to the differences in the samples themselves and the sequencing depth, the data of each sample were homogenized before analysis to facilitate the analysis of bacterial community diversity.

Four α-diversity indices were calculated using QIIME2 software to characterize the diversity of the bacterial community, Chao1, Shannon, Simpson and Pielou indices, respectively.The larger the Chao1 index, the more species are present in the bacterial community.The larger the Shannon and Simpson indices, the higher the diversity of the bacterial community, and the more uniformly distributed the species are. The larger the Pielou index, the more uniform the distribution of species. The specific formula is as follows:

$$Chao1 = Sobs + \frac{n_1(n_{1-1})}{2(n_2 - 1)} \tag{4}$$

$$Shannon = -\sum_{i=1}^{ASVs} P_i \log_e P_i \tag{5}$$

$$Simpson = 1 - \sum_{i=1}^{ASVs} P_i^2 \tag{6}$$

$$Pielou = \frac{Shannon}{\log_e ASVs} \tag{7}$$

where Sobs is the number of observed ASVs: n_1 is the number of ASVs with only 1 sequence: n_2 is the number of ASVs with only 2 sequences: P_i is the relative abundance of species i.

Species composition analysis is an important aspect of microbial community analysis, based on the results of taxonomic analysis, we can know the species composition of different groups or samples at each taxonomic level (Domain, Phylum, Class, Order, Family, Geues, Species). By sequencing and annotating the microbial community samples, we can obtain the species composition of the microbial community, the types and abundance of the species present in the community, based on which we can compare the structure of the composition of different microorganisms to obtain information on the differences of different microbial communities, whether the overall microbial composition is different or not, as well as the pattern of change in the structure of the community.

VI. Results and discussion

VI. A. Raman Spectroscopy Test

The Raman spectrograms of the prepared graphene oxide and the reduced graphene oxide solution were tested in the range of 0-2500 cm^{-1}, and the results are shown in Fig. 1. The Raman spectra of graphene-like substances contain two characteristic bands: the G band (~1596 cm^{-1}) formed by the ring-symmetric telescopic vibration of sp^2 atoms, and the D band (~1355 cm^{-1}) formed due to the ring-symmetric telescopic vibration of sp^2 atoms. As can be clearly seen from Fig. 1, the intensity ratio (ID/IG) of the D and G bands of reduced graphene oxide is significantly larger than that of oxidized graphene, indicating that the reduced graphene oxide has an increased number of sp^2 regions in the plane. From this, it can be judged that the experimentally prepared graphene oxide was obtained as reduced graphene oxide after hydrazine reduction.

Raman spectra of different electrodes (test range 0–2500 cm^{-1}) are shown in Figure 2. The CF electrode exhibits two weak peaks at 1358 cm^{-1} and 1614 cm^{-1}, corresponding to the D and G peaks reported in the literature at 1355 cm^{-1} and 1596 cm^{-1}, respectively. The D peak is attributed to the symmetric stretching vibration of sp^2 atomic rings, while the G peak originates from the stretching of all sp^2 bonds on the chains and rings. The PPy-CF electrode exhibits peaks at 938, 972, 1062, and 1426 cm^{-1}, corresponding to ring deformation associated with cationic radicals, ring deformation associated with di-cationic radicals, C-H plane deformation, and C-M stretching, respectively, indicating the presence of PPy-like substances adsorbed on the electrode surface; The rGO/PPy-CF electrode and GO/PPy-CF electrode both exhibit peaks corresponding to the PPy-CF peak wavelengths, with strong peaks appearing at 1335 and 1322 cm^{-1}, respectively, confirming the presence of graphene and polypyrrole on the surfaces of both electrodes. Additionally, both the rGO/PPy-CF electrode and the GO/PPy-CF electrode exhibit multiple peaks for PPy-CF, and the peak band data has shifted. This is due to the presence of π-π bond interactions between graphene and polypyrrole, which confirms that the surfaces of the rGO/PPy-CF electrode and the GO/PPy-CF electrode contain rGO/PPy and GO/PPy composite materials.

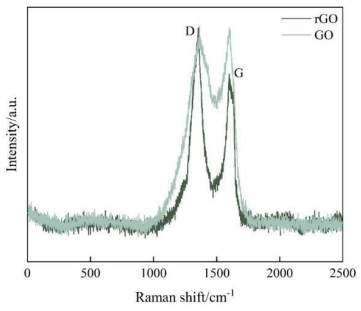

Figure 1: Raman spectra of graphene oxide and reduced graphene oxide

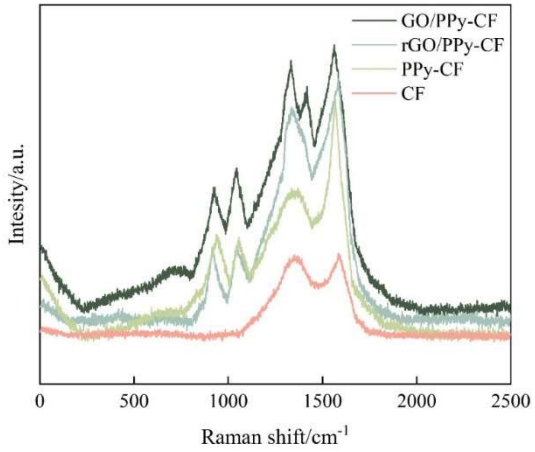

Figure 2: Raman spectra of different electrodes

VI. B. Mechanism of extracellular electron transfer in CGs anodized MFCs

In microbial fuel cells, two main electron transfer mechanisms exist: direct electron transfer facilitated by cytochromes or nanowires and indirect electron transfer mediated by electron shuttles. Bacteria close to the electrode surface can transfer electrons directly to the anode via nanowires or cytochromes, whereas those within the biofilm but not in close proximity utilize the dielectric or nanowire network for electron transfer over longer distances. Both pathways play a crucial role in power generation and organic utilization. In order to reveal the inner workings of how CGs anodes improve MFC performance, we conducted experiments to delve into the mechanism of extracellular electron transfer (EET). Electrochemical impedance spectroscopy (EIS) measured the overall electron transfer resistance of the biofilm after its formation on the electrode. The experiments were performed in fresh anode solution and the results are shown in Figure 3. The experimental results showed that the charge transfer resistance (R_{ct}) of each anode increased after biofilm formation. Notably, the CG-1000 had the highest electrical conductivity with an R_{ct} of 17.05 Ω, which was only 19.4% of the R_{ct} of the CC anode (87.95 Ω). The lower R_{ct} indicates a faster rate of extracellular electron transfer, possibly due to direct and indirect EET acceleration within the biofilm.

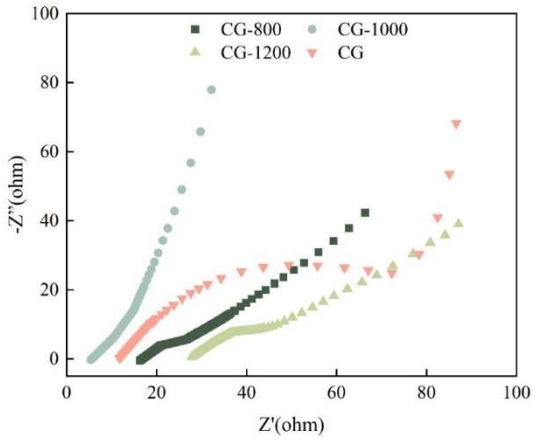

Figure 3: Nyquist curves of CGs and CC anodes covered by biofilms in fresh anolyte

For a deeper understanding of EET, cyclic voltammetry (CV) is shown and differential pulse voltammetry (DPV), performed in fresh anode solution using turnover mode, allowed for rapid recovery of cytochromes during scanning.The CV curves and DPV curves are shown in Fig. 4, Fig. 4 (a) The CV curves show clear redox pairs, with oxidizing and reducing peaks around -0.3V, attributed to the electrochemical activity of the cytochromes of the bacteria. The charge per unit area was calculated from the integral area enclosed by the anode CV curve in the order of CG-1000 (15.06 mC) > CG-1200 (12.87 mC) > CG-800 (7.53 mC) > CC (4.23 mC). This order indicates that higher redox active substances are present in the biofilm of CG anode and CG-1000 exhibits superior electron transfer performance.DPV is less affected by capacitive current and was used to further investigate the electron transfer mechanism. Figure 4 (b) shows a wide range of redox peaks with anodic potentials ranging from -0.35 V

to -0.38 V and cathodic potentials ranging from -0.32 V to -0.36 V. The CG anode exhibited a higher current density in the DPV test.

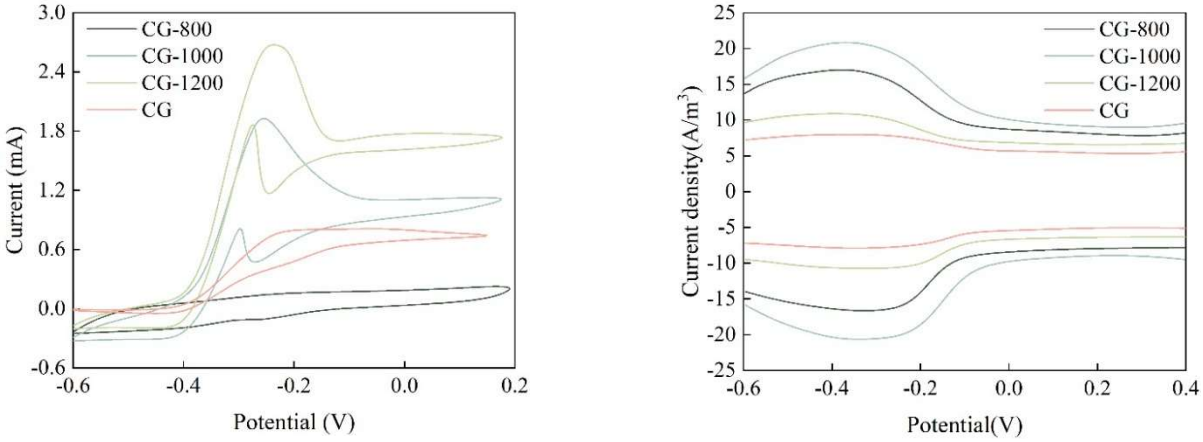

(a) CVs (b) DPVs

Figure 4: CVs and DPVs

To verify the mediated electron transfer (MET) process, electron mediator retention experiments were performed on these reactors. After the completion of the last cycle, the influent water is replaced to provide a new substrate for the microorganisms, and the voltage gradually returns to the maximum value. In this process, both direct electron transfer (DET) and MET play a role in electron transport, but MET relies more on bulk solutions because the medium is soluble and takes time to accumulate. Therefore, when the anode solution is renewed immediately after the MFC reaches its maximum voltage, there are sufficient nutrients for the bacteria to metabolize and generate electricity, but only a small amount of medium is present in the new anolyte. The evaluation of MET based on voltage fluctuations is shown in Figure 5. After the anode fluid is restored, the voltage of the different anodes is first reduced and then returns to the original level. During this process, the voltage of the CC anode drops to 0.43V and it takes 2.2 hours to return to the 0.65V plateau voltage. The CG-800 and CG-1200 use 1.85h and 1.96h to reach 0.67V and 0.69V respectively. The CG-1000 is negatively fluctuating. After a few minutes, its voltage reached 0.74V, which is 14% higher than the CC anode. CG anodes, especially CG-1000 anodes, exhibit excellent electron transfer mediation and fast MET rates.

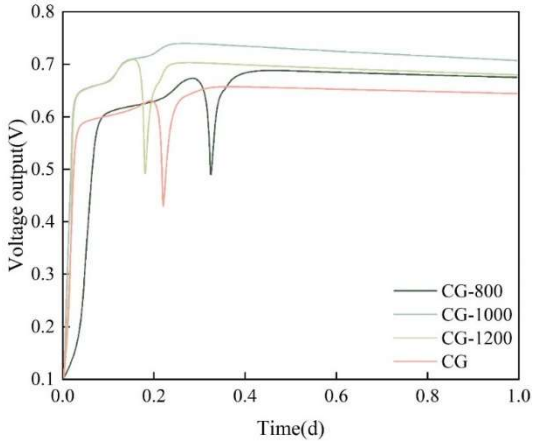

Figure 5: Voltages fluctuation

VI. C. Effect of Modified Anodes on Perchlorate Reduction

The initial concentration of perchlorate in the simulated wastewater was 150 mg/L, and the degradation of perchlorate by four different methods of modified anode MFC is shown in Figure 6. Figure 6 shows that compared with R/CC modified anode MFC, R+GNS/CC, R+MWCNT/CC, and R+GNS+MWCNT/CC modified anode MFC

significantly accelerated the degradation of perchlorate.R/CC alone modified anode MFC removed 84.1% of perchlorate with a degradation rate of 9.0 mg/h at 14 h, while R+GNS/CC, R+MWCNT/CC, R+GNS/CC, R+GNS/CC, R+GNS/CC, and R+GNS+MWCNT/CC modified anode MFC degraded perchlorate significantly. R+GNS/CC, R+MWCNT/CC, and R+GNS+MWCNT/CC jointly modified anode MFC had been completely degraded at 13, 12, and 10 h, respectively, with degradation rates of 11.5, 12.5, and 15 mg/h, respectively, which were increased by 27.8%, 38.9%, and 66.7%, respectively, when compared with the electrodes not modified with multi-walled carbon nanotubes and graphene. . The removal rates of pollutant perchlorate were all increased by anode-modified MFCs compared to blanks, which was attributed to the fact that graphene and multi-walled carbon nanotubes increased microbial attachment to the anode and facilitated electron transfer, thus accelerating the degradation of perchlorate.

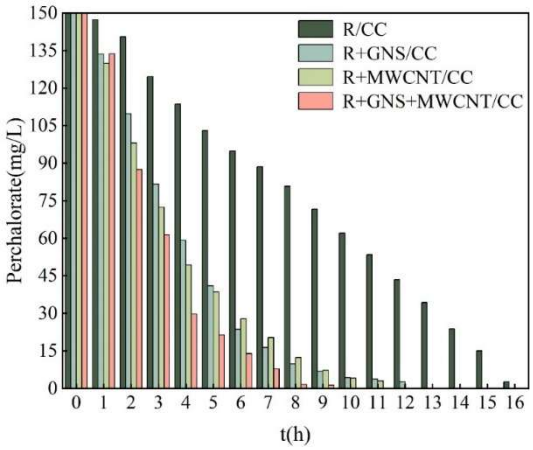

Figure 6: The perchlorate decrease of MFC with four different methods of modification anode

VI. D. Effect of Modified Anodes on MFC Electrical Producing Properties

In this experiment, the power generation performance of the MFC is measured by the output voltage. The output voltage of the anode MFC modified by R/CC, R GNS/CC, R MWCNT/CC, R GNS MWCNT/CC is shown in Figure 7, and the voltages are stable at 47, 77, 122 and 230mV, respectively, compared with the R/CC modified anode MFC, the output voltages of the anode MFC modified by R GNS/CC, R MWCNT/CC, R GNS MWCNT/CC are increased by 63.83%, 159.57%, 389.36%. As can be seen in Figure 7, there is a sudden change in voltage after the 0h water ingress, but it does not reach its stable level. After 2~3h, the reactor operation reaches a stable state, and the output voltage reaches a stable value, that is, the maximum output voltage value. The MFC output voltage is affected by factors such as electron donors, substrate conversion rate, number and activity of electrochemically active bacteria, and the effect of cell membranes on diffusion and mass transfer. At 8~10h, the MFC output voltage also decreases due to the decrease in the concentration of sodium acetate in the electron donor. The experimental results show that the co-modification of the anode by multi-walled carbon nanotubes and graphene-cobalt composites has a more obvious effect on the promotion of MFC power generation.

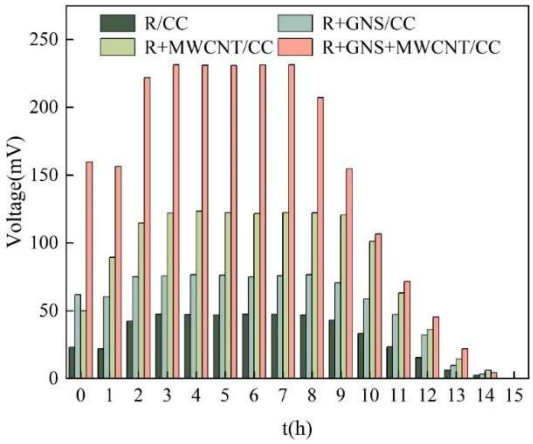

Figure 7: The output voltage of MFC with four different methods of modification anode

VI. E. Modified Anode Attachment Microorganism EPS Analysis

By extracting and analyzing the EPS of microorganisms attached to the carbon cloth of MFC anodes treated by four different methods, the results are shown in Fig. 8: Compared with R/CC, the extracellular proteins and DAN of microorganisms of the anodes obtained by three different treatments increased to different degrees, and polysaccharides decreased. The synergistic modification of MFC anode by graphene, multi-walled carbon nanotubes and multi-walled carbon nanotubes and cobalt graphene composites increased the amount of microorganisms adhering to the anode, thus increasing the number of electroproducing bacteria to a certain extent and further improving the electroproducing performance of the MFC, and secondly, polysaccharides are the main constituents of the EPS as shown in Fig. 8, and it has also been reported in the literature that polysaccharides are negatively charged, and the electron generated by the electroproducing bacteria degrading the substrate was transferred to the surface of the electrode by the microorganisms are transferred to the electrode surface, the same-sex charges repel each other, and polysaccharides will hinder the transfer of electrons, thus increasing the resistance of the electron transfer process.

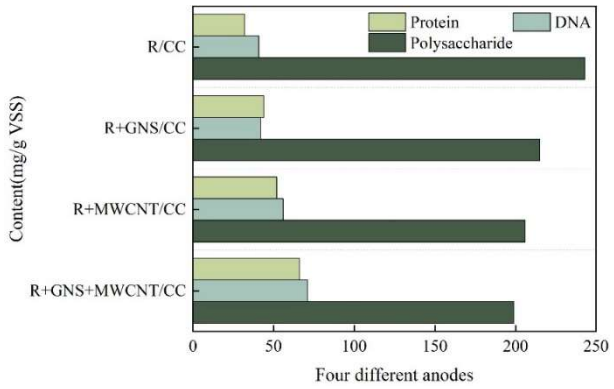

Figure 8: The analysis of EPS with four different methods of modification

VII. Conclusion

In order to understand the transfer characteristics of graphene-cobalt composites in the process of modified microbial fuel cell anode power generation, the authors designed numerical experiments to investigate the role of graphene-cobalt composites on the microbial fuel cell anode power generation by using electrochemical analytical test methods and microbial analysis.

(1) The CF electrode has two weak peaks (1358 cm^{-1} and 1614 cm^{-1}), corresponding to the D (1355 cm^{-1}) and G peaks (1596 cm^{-1}), respectively. pPy-CF electrode has four peaks (938, 972, 1062, and 1426 cm^{-1}), and the electrode surface has a PPy-like substance attached to the electrode. rGO/PPy-CF electrode and GO/ PPy-CF electrodes have corresponding peaks near the wavelength of the PPy-CF outgoing peaks, and there are strong peaks at 1335 and 1322 cm^{-1}, respectively, with graphene and polypyrrole present on the surface of both electrodes.

(2) When the biofilm was formed, the charge transfer resistance (R_{ct}) of each anode increased. Among them, the CG-1000 had the highest conductivity of 17.05 Ω and the CC anode had a conductivity of 87.95 Ω. The oxidation and reduction peaks were around -0.3 V. The CG-1000 had the best electron transfer performance. The anodic potential ranges from -0.35 V to -0.38 V and the cathodic potential ranges from -0.32 V to -0.36 V. The CG anode exhibits higher current density. After recovery of the anodic liquid, the voltage first decreased and then recovered.

(3) The MFC degradation rates of R/CC, R+GNS/CC, R+MWCNT/CC, and R+GNS+MWCNT/CC modified anodes were 9.0, 11.5, 12.5, and 15 mg/h, respectively. The MFC output voltages of the anodes modified by the four methods were stabilized at 47, 77, 122, and 230 mV. Compared with R/CC, the last three different treatments obtained anodic microorganisms had increased extracellular proteins and DAN and decreased polysaccharides, which increased the number of electroproducing bacteria and improved the MFC electroproduction performance.

Funding

This research was supported by the General Project of Basic and Applied Basic Research of Guangzhou Science and Technology Bureau in 2023 (Doctoral Young Science and Technology Personnel Category) (Project Number: SL2022A04J01326).

References

[1] Das, D. (2018). Microbial fuel cell. Auflage: Springer-Verlag GmbH.

[2] Santoro, C., Arbizzani, C., Erable, B., & Ieropoulos, I. (2017). Microbial fuel cells: From fundamentals to applications. A review. Journal of power sources, 356, 225-244.
[3] Gude, V. G. (2016). Wastewater treatment in microbial fuel cells–an overview. Journal of cleaner production, 122, 287-307.
[4] Boas, J. V., Oliveira, V. B., Simões, M., & Pinto, A. M. (2022). Review on microbial fuel cells applications, developments and costs. Journal of Environmental Management, 307, 114525.
[5] Tharali, A. D., Sain, N., & Osborne, W. J. (2016). Microbial fuel cells in bioelectricity production. Frontiers in Life Science, 9(4), 252-266.
[6] Li, M., Zhou, M., Tian, X., Tan, C., McDaniel, C. T., Hassett, D. J., & Gu, T. (2018). Microbial fuel cell (MFC) power performance improvement through enhanced microbial electrogenicity. Biotechnology advances, 36(4), 1316-1327.
[7] Dumitru, A., & Scott, K. (2016). Anode materials for microbial fuel cells. In Microbial electrochemical and fuel cells (pp. 117-152). Woodhead publishing.
[8] Kong, S., Zhao, J., Li, F., Chen, T., & Wang, Z. (2022). Advances in anode materials for microbial fuel cells. Energy Technology, 10(12), 2200824.
[9] Narayanasamy, S., & Jayaprakash, J. (2021). Carbon cloth/nickel cobaltite (NiCo2O4)/polyaniline (PANI) composite electrodes: Preparation, characterization, and application in microbial fuel cells. Fuel, 301, 121016.
[10] Islam, A. K., Dunlop, P. S., Bhattacharya, G., Mokim, M., Hewitt, N. J., Huang, Y., ... & Brandoni, C. (2023). Comparative performance of sustainable anode materials in microbial fuel cells (MFCs) for electricity generation from wastewater. Results in Engineering, 20, 101385.
[11] Sonawane, J. M., Yadav, A., Ghosh, P. C., & Adeloju, S. B. (2017). Recent advances in the development and utilization of modern anode materials for high performance microbial fuel cells. Biosensors and bioelectronics, 90, 558-576.
[12] Mahalingam, S., Ayyaru, S., & Ahn, Y. H. (2021). Facile one-pot microwave assisted synthesis of rGO-CuS-ZnS hybrid nanocomposite cathode catalysts for microbial fuel cell application. Chemosphere, 278, 130426.
[13] Rani, G., Jaswal, V., & Yogalakshmi, K. N. (2023). Anode modification: An approach to improve power generation in microbial fuel cells (MFCs). In Development in wastewater treatment research and processes (pp. 133-152). Elsevier.
[14] Yang, W., Chata, G., Zhang, Y., Peng, Y., Lu, J. E., Wang, N., ... & Chen, S. (2019). Graphene oxide-supported zinc cobalt oxides as effective cathode catalysts for microbial fuel cell: High catalytic activity and inhibition of biofilm formation. Nano Energy, 57, 811-819.
[15] Tan, L., Pan, Q. R., Wu, X. T., Li, N., Song, J. H., & Liu, Z. Q. (2019). Core@ Shelled Co/CoO embedded nitrogen-doped carbon nanosheets coupled graphene as efficient cathode catalysts for enhanced oxygen reduction reaction in microbial fuel cells. ACS Sustainable Chemistry & Engineering, 7(6), 6335-6344.
[16] Tiwari, S. K., Sahoo, S., Wang, N., & Huczko, A. (2020). Graphene research and their outputs: Status and prospect. Journal of Science: Advanced Materials and Devices, 5(1), 10-29.
[17] Pareek, A., Sravan, J. S., & Mohan, S. V. (2019). Fabrication of three-dimensional graphene anode for augmenting performance in microbial fuel cells. Carbon Resources Conversion, 2(2), 134-140.
[18] D Ghuge, A., R Shirode, A., & J Kadam, V. (2017). Graphene: a comprehensive review. Current drug targets, 18(6), 724-733.
[19] Ye, R., & Tour, J. M. (2019). Graphene at fifteen. ACS nano, 13(10), 10872-10878.
[20] Liu, Z., Ge, B., Li, K., Zhang, X., & Huang, K. (2016). The excellent performance and mechanism of activated carbon air cathode doped with different type of cobalt for microbial fuel cells. Fuel, 176, 173-180.
[21] Aiswaria, P., Mohamed, S. N., Singaravelu, D. L., Brindhadevi, K., & Pugazhendhi, A. (2022). A review on graphene/graphene oxide supported electrodes for microbial fuel cell applications: Challenges and prospects. Chemosphere, 296, 133983.
[22] Li, L., Liu, S., Wang, H., & Yang, P. (2018). Application of graphene-cobalt/nickel composite-carbon cloth modified electrode in microbial fuel cell. Environmental Engineering Science, 35(11), 1173-1184.
[23] Yu, F., Wang, C., & Ma, J. (2016). Applications of graphene-modified electrodes in microbial fuel cells. Materials, 9(10), 807.
[24] Yuan, H., & He, Z. (2015). Graphene-modified electrodes for enhancing the performance of microbial fuel cells. Nanoscale, 7(16), 7022-7029.
[25] Yaqoob, A. A., Ibrahim, M. N. M., Yaakop, A. S., Umar, K., & Ahmad, A. (2021). Modified graphene oxide anode: a bioinspired waste material for bioremediation of Pb2+ with energy generation through microbial fuel cells. Chemical Engineering Journal, 417, 128052.
[26] Paul, D., Noori, M. T., Rajesh, P. P., Ghangrekar, M. M., & Mitra, A. (2018). Modification of carbon felt anode with graphene oxide-zeolite composite for enhancing the performance of microbial fuel cell. Sustainable Energy Technologies and Assessments, 26, 77-82.
[27] Liu, Z., Zhou, L., Chen, Q., Zhou, W., & Liu, Y. (2017). Advances in graphene/graphene composite based microbial fuel/electrolysis cells. Electroanalysis, 29(3), 652-661.
[28] Starowicz, A., Zieliński, M., Rusanowska, P., & Dębowski, M. (2023). Microbial fuel cell performance boost through the use of graphene and its modifications. Energies, 16(2), 576.
[29] Fu, L., Wang, H., Huang, Q., Song, T. S., & Xie, J. (2020). Modification of carbon felt anode with graphene/Fe 2 O 3 composite for enhancing the performance of microbial fuel cell. Bioprocess and Biosystems Engineering, 43, 373-381.
[30] Nosek, D., Mikołajczyk, T., & Cydzik-Kwiatkowska, A. (2024). Enhancing microbial fuel cell performance: anode modification with reduced graphene oxide and iron (III) for improved electricity generation. Clean Technologies and Environmental Policy, 1-18.
[31] Zhang, Y., Liu, L., Van der Bruggen, B., & Yang, F. (2017). Nanocarbon based composite electrodes and their application in microbial fuel cells. Journal of Materials Chemistry A, 5(25), 12673-12698.
[32] Meladi L. Motloutsi,Funeka Matebese,Mashawe J. Madito,Mxolisi M. Motsa,Muthumuni Managa & Richard M. Moutloali. (2025). Zwitterion functionalized graphene oxide thin film nanocomposite membrane for brackish water desalination and natural organic matter removal. Desalination and Water Treatment,323,101276-101276.
[33] Zaman Badrus & Wisnu Wardhana Irawan. (2018). Potential of Electric Power Production from Microbial Fuel Cell (MFC) in Evapotranspiration Reactor for Leachate Treatment Using Alocasia macrorrhiza Plant and Eleusine indica Grass. E3S Web of Conferences,31,02010-02010.
[34] Bojian Fan,Yuhang Xin,Yingshuai Wang,Qingbo Zhou,Shaowen Huang,Kunyu Zhao... & Hongcai Gao. (2025). Ultrathin carbon layer-engineered spherical hard carbon anodes with high initial Coulombic efficiency and kinetic-enhanced sodium storage. Chemical Engineering Journal,517,164319-164319.
[35] Ning Chen,Xu Zhao,Yu Zhou,Yihang Xie,Yujiang He,Chunhua Yang & Weihua Gui. (2025). Electrochemical impedance spectroscopy online measurement method for lithium-ion batteries based on correlation detection and improved Levenberg-Marquardt algorithm. Measurement,255,117995-117995.